

Geomechanical prestack depth migration of the Kraken 3D (Browse Basin, Australia)

Jarrold Dunne*
Karoon Gas Australia
jdunne@karoongas.com.au

Matthew Zengerer
Gondwana Geoscience
matt@gondwanageo.com

Hamish Stein
University of Melbourne
hamish.stein@gmail.com

Stephen Gallagher
University of Melbourne
sigall@unimelb.edu.au

Ferudun Kilic
Paradigm Geophysical
Ferudun.Kilic@PDGM.com

Pramod Kumar
Paradigm Geophysical
Pramod.Kumar@PDGM.com

Shiv Pujan Singh
Paradigm Geophysical
Shiv.Singh@PDGM.com

SUMMARY

Conventional pre-stack depth migration applied to the broadband Kraken 3D Marine Seismic Survey was unable to fully resolve short-wavelength velocity anomalies below the sea floor causing obvious imaging problems and limiting depth conversion and amplitude interpretation. Improved imaging was achieved by initiating tomography using a velocity model built by combining geomechanics with rock physics appropriate for shallow carbonates and mudrocks.

3D gravity modelling using high-resolution bathymetry and compaction trends constitutes a new approach for iteratively building a 3D geomechanical model. Effective stress is derived by applying Terzaghi's principle within an integration (along depth) involving the model bulk and fluid densities and the vertical component of gravity (all of which may vary spatially, using more refined models).

Carbonate and mudrock rock physics models, believed to be appropriate for Neogene sediments along much of the NW Shelf of Australia were derived from abundant core and wireline data acquired during the recent IODP Expedition 356. These models provide the necessary link between effective stress and P-wave velocity with Backus averaging handling the "seismic scale" mixing of different lithologies expected in the Kraken 3D area.

Kirchhoff prestack depth migration was revisited from archived preprocessed gathers using the geomechanical model combined with Common reflection angle gathers (CRAM) to initiate tomography. CRAM gathers were very effective in the presence of multiples and complex near surface topography to achieve a better update in tomography. Heavy smoothing of velocities was imposed where sequence stratigraphic interpretation suggests only distal mudstone facies. Tomography in shallower layers was then revisited to restore geologically plausible depth structures and deliver a clear improvement in imaging relative to previous processing efforts.

Key words: Geomechanical, pre-stack depth migration, rugose sea floor, carbonate rock physics, IODP, Browse basin, Seringapatam Sub-basin, Caswell Sub-basin.

INTRODUCTION

The broadband Kraken 3D Marine Seismic Survey was acquired in 2013 to image a prominent structural high overlain by a highly rugose sea floor on the outermost edge of the Browse basin (Figure 1). Prestack time migration was immediately followed by 5 iterations of Kirchhoff prestack depth migration and some cosmetic postprocessing. Despite many examples of clear imaging improvements following the PSDM, there were also some obvious areas where poor imaging remained and where interval velocities didn't make much geological sense (Dunne, 2016).

An intriguing drilling prospect was identified containing possible Paleocene turbidites onlapping a Permo-Triassic structural high. However, there remained a strong imprint of the sea floor profile and the Tertiary carbonate overburden on amplitude maps at the target level. Combined with limited accuracy in depth conversion, to date there has been insufficient evidence of reservoir presence and hydrocarbon porefill to adequately derisk the prospect and attract a drilling partner.

Improved imaging was sought by revisiting the tomography using an initial velocity model built by combining geomechanical principles with rock physical models that are appropriate for shallow carbonates and mudrocks. The seeds for these ideas came from two seemingly unlinked sources. The first was a conference paper on geomechanical PSDM (Birdus, 2008) and the second came via professional associations with researchers at Melbourne University involved in the International Ocean Drilling Program (IODP).

For commercial reasons, the "Birdus" paper was deliberately non-specific on the mathematics behind the geomechanical approach used, but the case studies from similar rugose shelf-break settings in the NW Shelf were impressive. The shape of velocity anomalies associated with sea floor slump canyons and isolated reef buildups resembled the gravity potential fields associated with terrain. Recognizing that effective pressure is the ultimate driver of the elastic properties (V_p , V_s , ρ) for a given rock, led to the idea that a 3D model of effective pressure could be built by computing the 3D effects of gravity and terrain, while also considering any lithological differences in the overburden. For use in seismic imaging, a geomechanical model such as this would also require relations between effective pressure and V_p , such as those that can be measured in tri-axial pressure cells in a laboratory (e.g., Lebedev, et al, 2013).

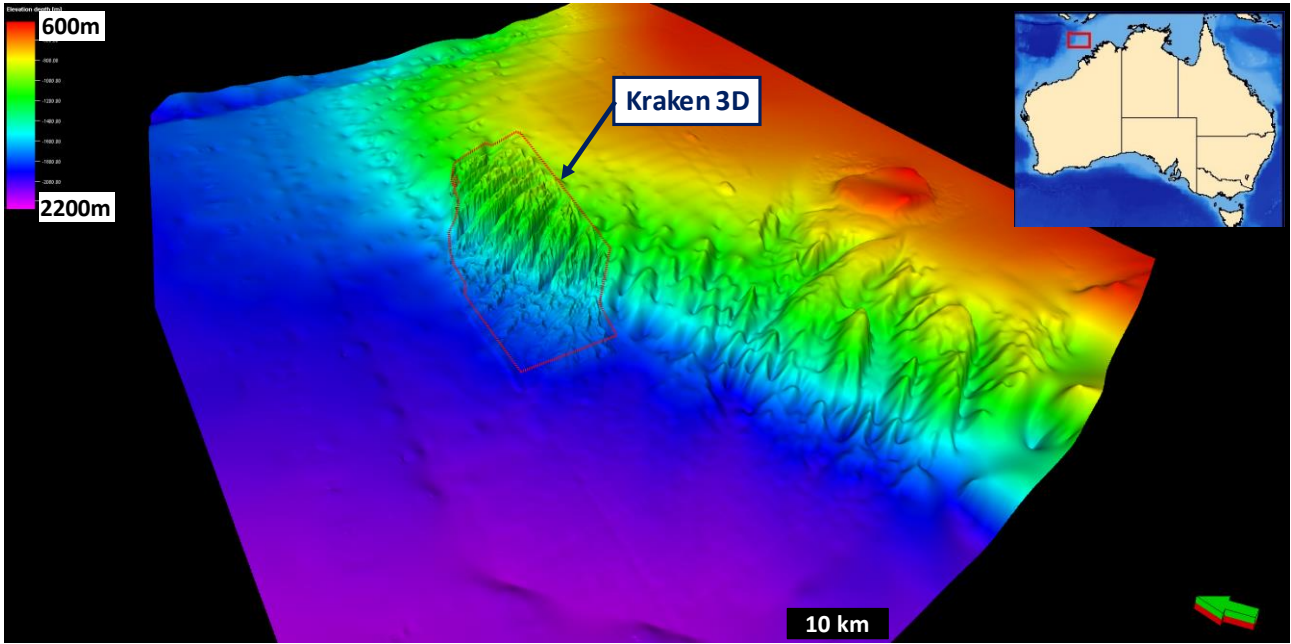


Figure 1. Location of the Kraken 3D and composite image of the highly rugose bathymetry from 2D and 3D seismic.

Prospective areas of the Australian continental shelf tend to have Tertiary carbonates in the overburden, which grade to marls and deepwater mudstones at the shelf slope break. This change in rheology is probably the reason for the shelf slope break because mudstones have a significantly lower angle of repose. However, such mudstones are difficult to sample, preserve and thus achieve valid tri-axial pressure cell tests. Also, there has been little interest in sampling shallow Tertiary carbonates because they rarely form viable hydrocarbon reservoirs.

Recent IODP drilling targeting Neogene carbonates in the NW Shelf offered a unique opportunity to build a database of (effective) pressure-dependent velocities that might be applied widely throughout adjacent basins (Figure 2). The holistic sampling approach employed by the IODP (Gallagher, et al., 2017) enabled different carbonate facies to be broken out with elastic properties measured to surface. Continuous coring enabled frequent sampling of porosity and therefore a near-continuous density profile could be built for each facies. This meant it would be possible to achieve an accurate integration (along depth) of density to compute the overburden stress. Effective pressure profiles could then be computed for the brine porefill and hydrostatic conditions encountered during drilling.

A separate study was spawned into the rock physics of shallow carbonates (Stein, 2017, MSc in progress), which are poorly understood given the focus on deeper-buried carbonate reservoirs of the Middle East and other regions. In such regions, the carbonates tend to have experienced significant chemical compaction and often behave with what can be referred to as “stiff” rock physics trends, mirroring the Voigt bound. Early findings from the IODP-based rock physics study suggest that “contact” models, mirroring the Reuss bound may be more appropriate for shallow carbonates, until sufficient calcite cement forms to fuse the grain framework of the rock.

We continue by discussing the mathematics “under the hood” of the geomechanical model, including details of the high-resolution 3D gravity model that must be built. An example of a carbonate rock physics model from the IODP program is then shown, although the exact details of how we built the initial V_P model for imaging in the Kraken 3D area will be kept proprietary. We discuss the main learnings from revisiting the Kirchhoff prestack depth migration using the geomechanical model as the starting point for tomography and finish by highlighting some of the impacts on seismic interpretation.

THE GEOMECHANICAL MODEL

3D gravity modelling using high-resolution bathymetry and density compaction trends is the core part of the geomechanical method proposed here. Detailed bathymetry (or terrain) maps obtained during modern seismic acquisition must be extended as accurately as possible outside of the survey area to avoid edge effects in modelling gravity. An initial model for sediment densities can be derived assuming mechanical compaction as the primary driver for porosity loss with depth below mudline (Athy, 1930):

$$\phi = \phi_0 e^{-kZ_{bml}}$$

where ϕ_0 is the depositional porosity, Z_{bml} is the depth below mudline and k is the compaction coefficient, followed by:

$$\rho_b(z) = \rho_{grain}(1 - \phi) + \rho_f(z).$$

where ρ_{grain} is a volume weighted average grain density and $\rho_f(z)$ is the density of brine.

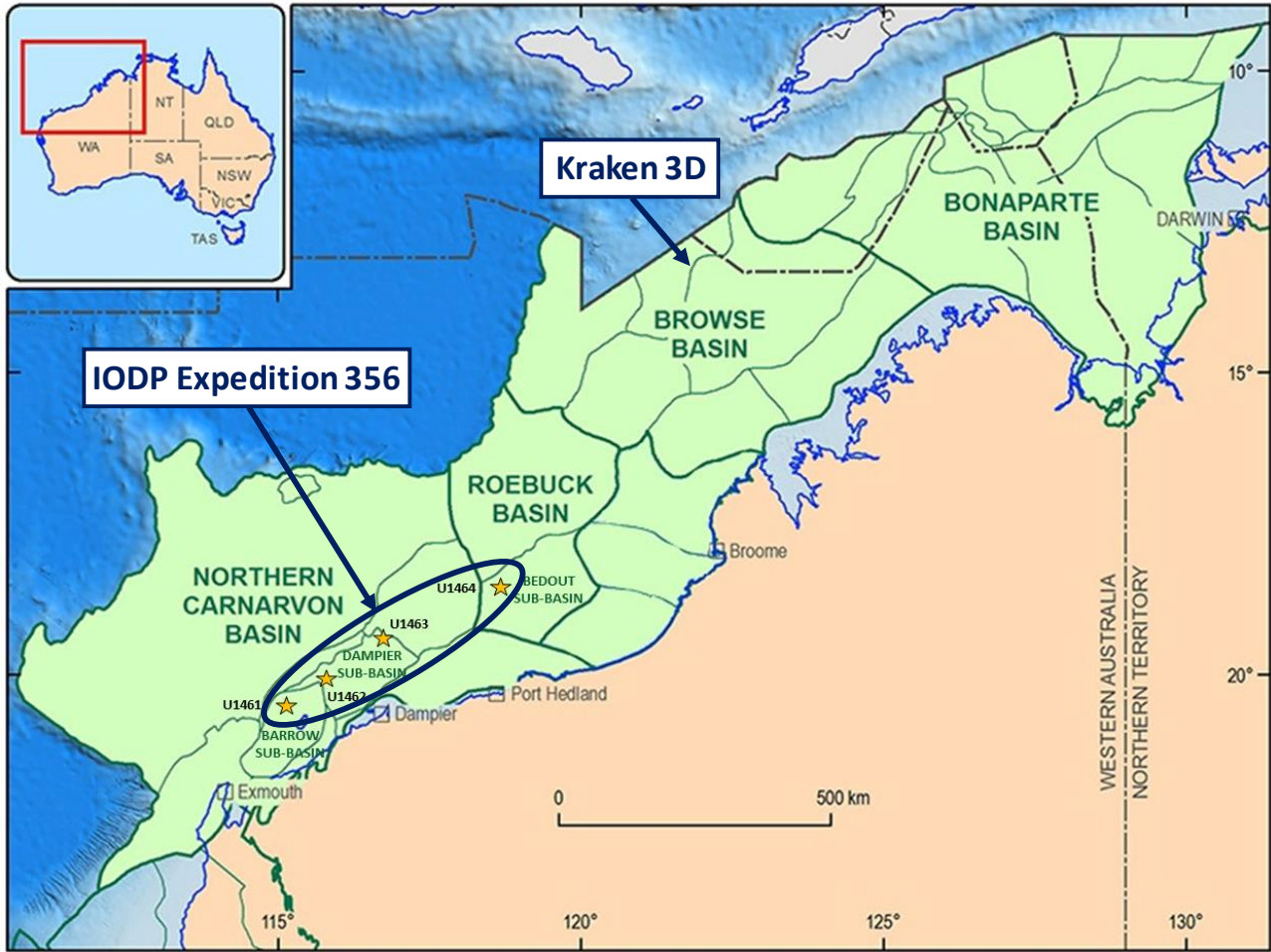


Figure 2. IODP Expedition 356 drilling sites and relationship to sedimentary basins of the greater North West Shelf (edited from Bernecker, et al., 2015). The Kraken 3D may lie more than 500km to the north but the sub-basins have similar burial histories and it should be possible to extrapolate rock physical knowledge long distances, especially for shallow sediments.

The GeoModeller software was used to compute the vertical component of gravity (g_z) for the density model described above, where compacting sediments are modelled below a uniform density water layer (Zengerer, 2016). At this stage, g_z must be computed using the Fast Fourier Transformation method, which is faster to run than the Spatial Convolution method but not as accurate unless large amounts of vertical padding are applied, thus requiring much more memory. Only the FFT method can currently output a 3D result, which is essential for achieving our goal of creating a 3D seismic V_P model.

We initially tested the method on a 2.5D model that was designed to represent a single idealized sea floor canyon. Results were compared between models built using a constant sediment density and using a compaction trend. When viewed as gravity gradients the results were quite different with the compaction trend model showing more complex and rapid lateral variations underneath the canyon.

Given memory and CPU limitations, the final model was computed on a 400x400x4m grid and output as a voxel. Figures 3 and 4 illustrate the vertical gravity and gravity gradient (g_{zz}) responses along a north-south section. The changes in the gravity field and gravity gradients are quite profound with respect to the submarine canyons. On the vertical gravity response, up to 30 mGal variability was noted at common depth values below and adjacent to the canyons. The gravity gradients show more complex shapes and to some extent appear to emulate the work of Birdus.

A 3D effective stress model is then derived using Terzaghi's principle (1936), which is widely regarded as appropriate for use with unconsolidated sediments. Hydrostatic conditions are typically assumed for the shallow overburden, but overpressures could also be accommodated in the method, in so far as they can be reliably estimated. The key innovation required implementing an integration (along depth, z) involving the model bulk and fluid densities and the vertical component of gravity (all of which may vary with x , y and z), according to the equation below:

$$P_{eff}(x, y, z) = \int_0^z [\rho_b(x, y, z)g_z(x, y, z) - \rho_f(x, y, z)g_z(x, y, z)]dz$$

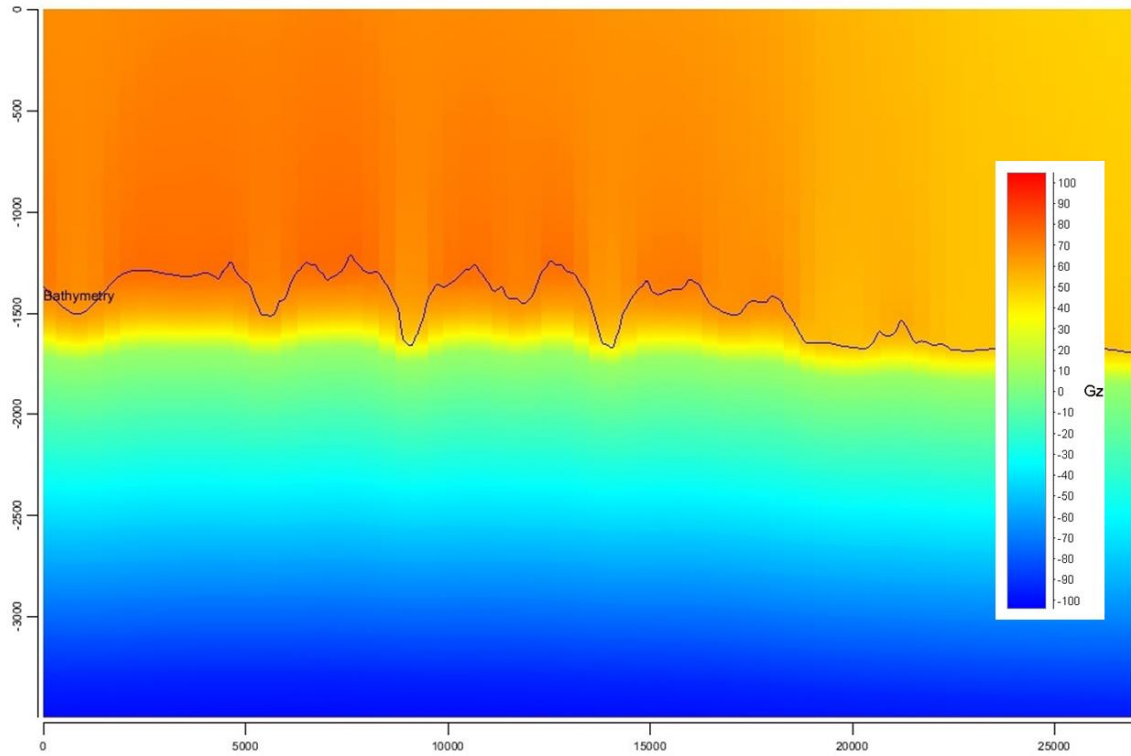


Figure 3. 2D north-south profile showing the vertical gravity g_z model response for a $400 \times 400 \times 4$ m grid, where up to 30 mGal variability can be observed at common depth values below and adjacent to the canyon bases.

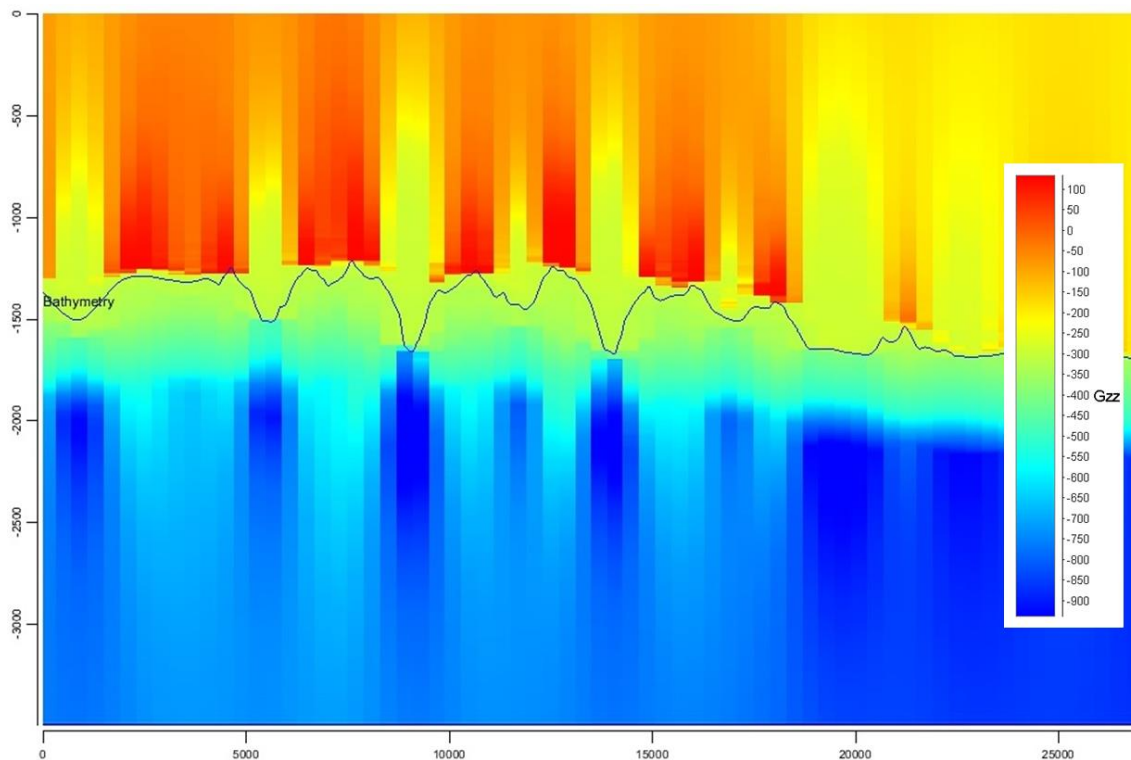


Figure 4. 2D north-south profile showing the vertical gravity gradient g_{zz} model response for a $400 \times 400 \times 4$ m grid highlighting the large variations expected either side of the canyons.

By applying a rock physics model to convert P_{eff} into V_P , this method constitutes a bridge between seismic and gravity data. As it currently stands, the method is essentially an iterative approach towards obtaining a fully integrated model of elastic properties using both seismic and gravity data. If gravity data (and in particular, gravity gradiometry data) are available then we could use the porosity

model hung from sea floor to generate an initial density model for use in a gravity inversion and then use the inverted densities to re-derive P_{eff} and then V_P .

Strictly speaking, porosity loss by mechanical compaction is also driven by P_{eff} , but this was deemed an unnecessary complication of the mathematics at this stage. In time, it may be possible to jointly invert for everything at once rather than the current boot-strapping approach. For now, it is regarded as a significant step up to perform gravity modelling in the way described above rather than with constant overburden densities (Gibson, et al., 2016).

SHALLOW CARBONATE ROCK PHYSICS

Carbonate and mudrock rock physics model, were derived from abundant core and wireline data acquired during the recent IODP Expedition 356 (Gallagher, et al, 2017). The expedition focussed on Neogene sediments at several sites in the NW Shelf of Australia but we believe the results should remain accurate for equivalent facies along much of the Westralian superbasin. Aside from the high quality geological and physical properties data acquired, the dataset provides a rare opportunity to study the rock physical behaviour of carbonates at and immediately after deposition.

Key elements of the rock physics study (Stein, 2017, in press) include: 1) preparation of the diverse geological information to enable accurate characterization of the carbonate facies associated with each physical data point; 2) preparation of core-based physical properties; 3) preparation (conditioning) of well-log based physical properties; 4) rock physics cross-plotting; and 5) determination of appropriate rock physics models for each significant carbonate facies.

Figure 5 shows the rock physics cross-plotting for the Packstone facies, with the linked-trend models driven by P_{eff} . As described earlier, P_{eff} was computed from the continuously-cored density data under some reasonable assumptions. The Packstone example covers a wide range of effective pressures, or depths (below mudline), with abundant V_P data and somewhat less V_S data surviving quality control. In this example, the Sun rock physics model (Sun, 2004) was tested and appears to give a reasonable quality fit.

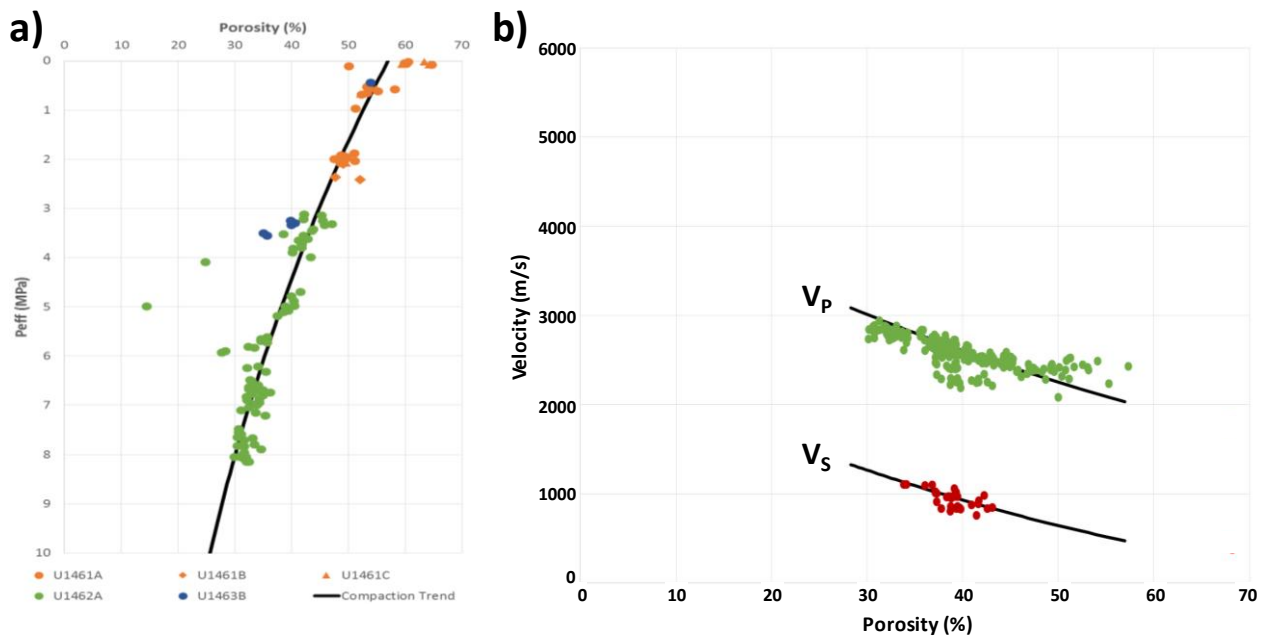


Figure 5. Well-log data and core data from IODP Expedition 356, focussing on the Packstone carbonate facies. Clear trends exist using data from several wells thus enabling linked rock physics trends to be formed using a) Athy’s compaction trend (driven by P_{eff}) and b) the Sun rock physics model.

Stein tested a wide range of rock physics models for carbonate facies ranging from mudstones to grainstones. For some facies it became clear that contact models offered a better fit to the data towards the depositional (or critical) porosity end of the crossplot. The high porosity behaviour is naturally of most interest to the problem of building shallow velocity models for imaging.

Stein’s findings suggest that calcite cements, whilst likely to exist shortly after deposition, may not fuse the grains together until the porosity reaches a (second) critical value. At this branch point, it may be necessary to switch to a stiffer rock physics model in order to model further porosity loss. For these lower porosity ranges, inclusion models may work better, or alternatively heuristic models that approach the Voigt or upper Hashin-Shtrikmann bounds.

Rock physics models, such as the one shown above, provide the necessary link between effective stress and P-wave velocity with Backus averaging handling the “seismic scale” mixing of different lithologies expected in the Kraken 3D area. The trick is to use

sequence stratigraphic principles to modulate the contribution of different carbonate facies and to make use of well log or VSP information when available for local calibration.

SEISMIC IMAGING AND INTERPRETATION IMPACT

CRAM (common reflection angle) angle domain imaging in combination of Kirchhoff prestack depth migration was revisited using the geomechanical model to initiate tomography. Preprocessed gathers were retrieved from the previous attempt at PSDM, which was conducted using a more traditional workflow. Given the common starting point, the only differences in the final results come from differences in the velocity model and in the post-processing.

To finalize the initial geomechanical model, sequence stratigraphic concepts were used to identify a discrete number of carbonate facies as most likely to represent the shallow overburden in the Kraken 3D area. The weightings used for Backus averaging of the rock physics trends for each carbonate facies were also adjusted to match nearby VSP data. Some further trial and error adjustment was required for sequences not encountered in any wells so far, such as a distal hemipelagic mudstone that thickens to the south-western side of the survey area.

Tomography proceeded in a top down manner initially, with only minor updates from the geomechanical model allowed in the two uppermost layers while the tomography was given freer rein in layers 3 and 4. False depth structures appeared in layer 4 which is interpreted as a distal mudstone or marly sequence based on its stratigraphic stacking patterns and seismic character. Such a sequence ought to have quite smooth lateral velocity variations, as it is buried relatively deeply and therefore much less sensitive to the effective pressure impact of the overlying sea-floor canyons.

Heavy smoothing of velocities was imposed in layer 4 to override the tomographic solution for this layer. Tomography in layer 3 was revisited to achieve flat gathers over layers 3 and 4 while ensuring geologically plausible depth structures in layer 4. This increased the lateral velocity variation within layer 3 relative to what was achieved by the first iteration of tomography within that layer. The largest changes occurred where shallow hydrocarbons are trapped (slow velocities); and where high-velocity carbonate grainstone facies are inferred from stacking patterns.

Tomography was then recommenced in layers 5 and 6, keeping in the mind the possibility of overpressuring in layer 5 which is interpreted as a hemipelagic mudstone. The difference between the initial geomechanical velocity model and the final velocity model highlighted the persistence of the stress-induced velocity anomalies in the immediate vicinity below the sea floor slump canyons. The difference between the final velocity model from this imaging project relative to the previous attempt at PSDM shows wholesale changes in most areas (Figure 6). Further work is ongoing to interpret the new velocity model in terms of its rock physics implications and with respect to over-pressuring, which is known to exist in this area.

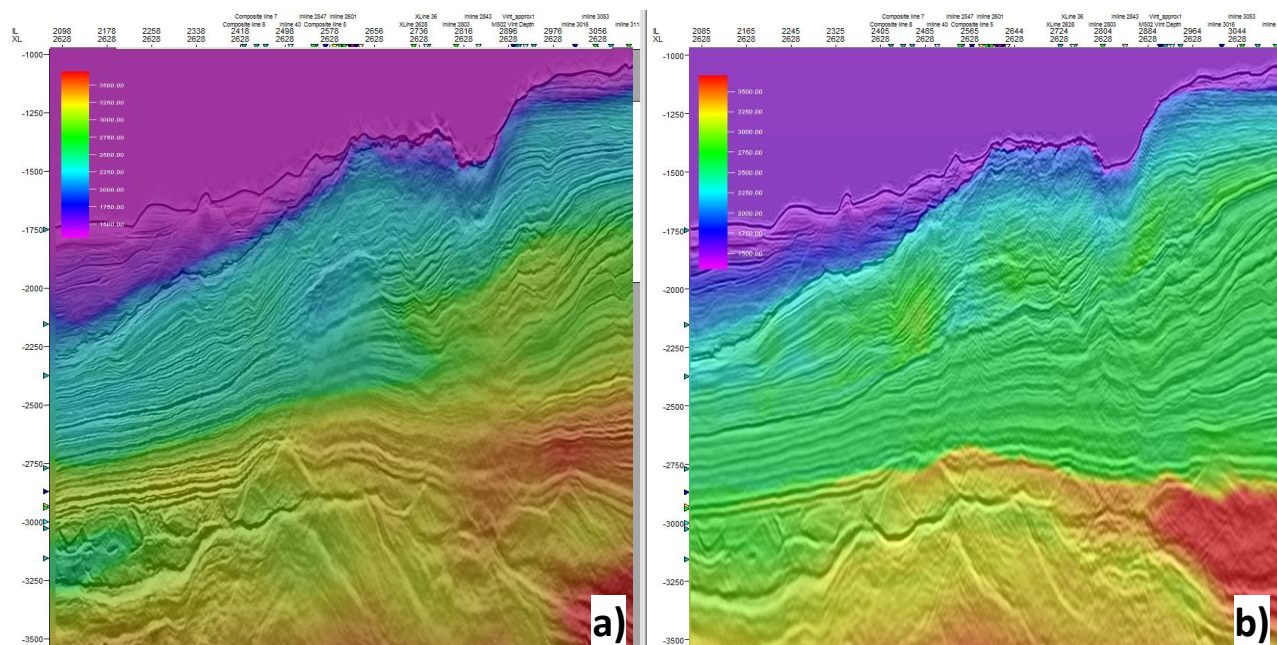


Figure 6. Final seismic interval velocities in depth for a) the previous PSDM processing; and b) the geomechanical PSDM. The geomechanical effect of the sea floor slump canyons persists for some distance into the model and strong lateral velocity variations are focussed into the prograding Tertiary grainstone carbonates, within which some shallow hydrocarbons appear to be trapped. Velocities below 3km appear to suggest strong overpressures within the Seringapatam sub-basin to the west.

Some spectral shaping was conducted after the migration to restore the frequency spectrum to a desired shape without overly boosting high frequency noise. In the previous migration the spectral shaping was perhaps slightly overdone resulting in some high

frequency sidelobes in some shallow sequences. In any case, we were unable to exactly match the frequency content of the initial processing, despite being satisfied that we had pushed the bandwidth to a level that was appropriate for the data.

Ignoring these cosmetic differences, the revised geomechanical PSDM appears to have achieved a clear improvement in imaging (Figure 7). Large areas of the 3D volume now show more sensible depth structures particularly towards the base of layer 4 where benign structuration is expected based on our regional understanding. The image appears more continuous, especially underneath the sea-floor slump canyons and the shallow hydrocarbon accumulations. The complex faulted structures within the Permo-Triassic now appear more consistent from fault block to fault block.

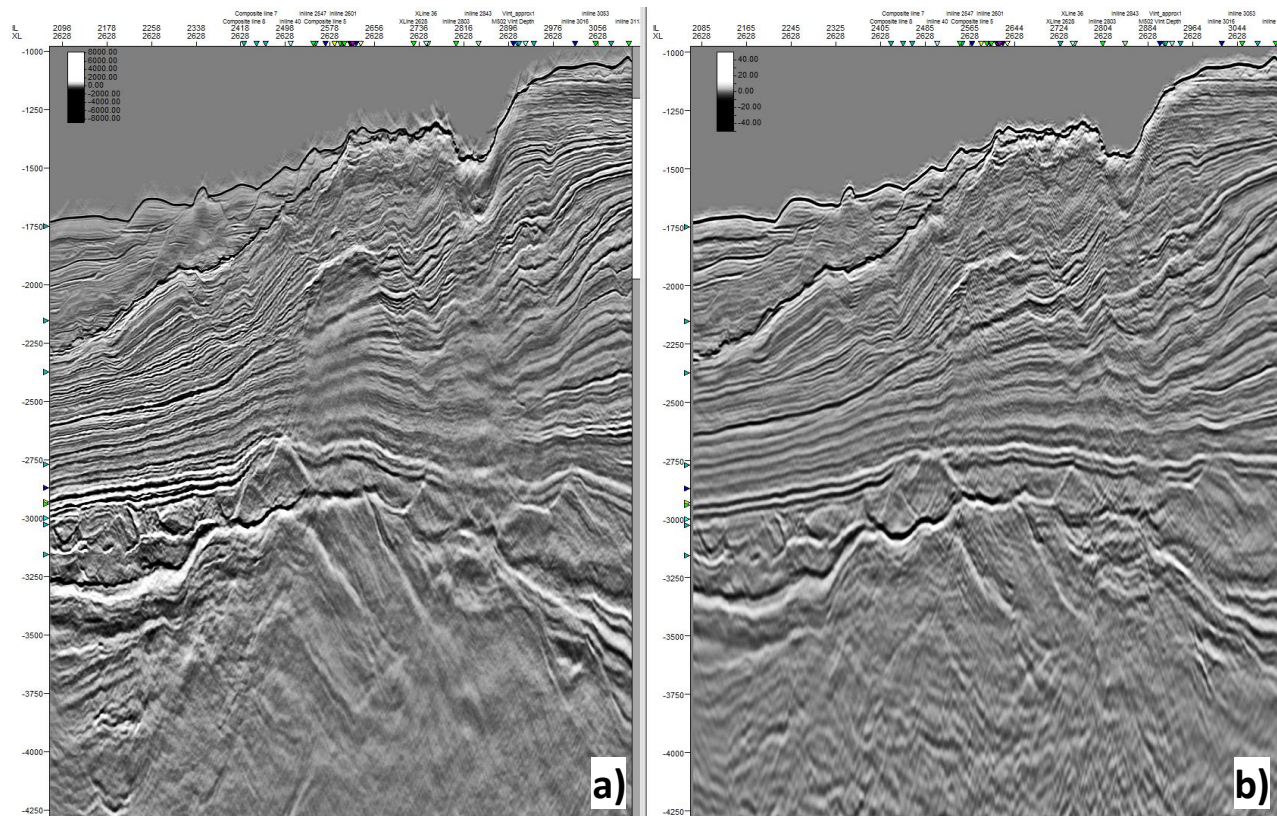


Figure 7. Final full-offset seismic image in depth for a) the previous PSDM processing; and b) the geomechanical PSDM. Distal mudstones and carbonates (at ~2.5-3.0km depths) now show sensible structures and more consistent seismic character.

Seismic interpretation is ongoing at the time of writing and future observations will undoubtedly arise, especially with respect to seismic amplitudes and AvO. An initial test of the amplitude integrity was conducted by extracting a RMS amplitude map over the entire interval represented by layer 4 (Figure 8a). The seismic stratigraphy of this interval indicates it is comprised almost entirely of distal facies, such as mudstones and marls. It is expected to have very uniform amplitudes overall and any lateral variations (when taken over a sizeable depth window) are likely to be subtle. The map extracted from the original PSDM (Figure 8b) shows a strong and clear trend of diminished illumination underneath the Miocene carbonate shelf break with even weaker amplitudes directly below the sea floor canyons. The same attribute extracted from the current PSDM (Figure 8c) appears almost entirely uniform, thereby suggesting that attempts to use AvO may not require illumination corrections this time around.

DISCUSSION

The method shown here has applications in other shelf edge permits but, as Birdus also indicated, it should also help to image under reefs where the opposite gravitational effect to a sea floor canyon occurs. It may also prove relevant to imaging near or below salt diapirs, because low density salt bodies will also create 3D stress effects that may be difficult to predict without proper modelling.

Seismic survey design parameters, such as the streamer length, and area specific factors, such as water depth, will also play a role in determining the relevance of this method to improving imaging. In some cases, it may be possible to achieve excellent results with tomography alone, or perhaps by using full-waveform inversion (FWI). However, even when these methods work well, it probably cannot hurt to build an initial velocity model using the geomechanical approach.

The method proposed here requires some investment of time and thought into compiling robust rock physics databases for overburden lithologies. However, this is something that probably should be done anyway for a myriad of other subsurface applications, for example in shallow hazard assessments. The method may have its origins in seismic imaging, but it also constitutes

a stepping stone towards joint seismic and gravity data inversions. Further research is needed into building common Earth models for fully integrating different geophysical exploration techniques.

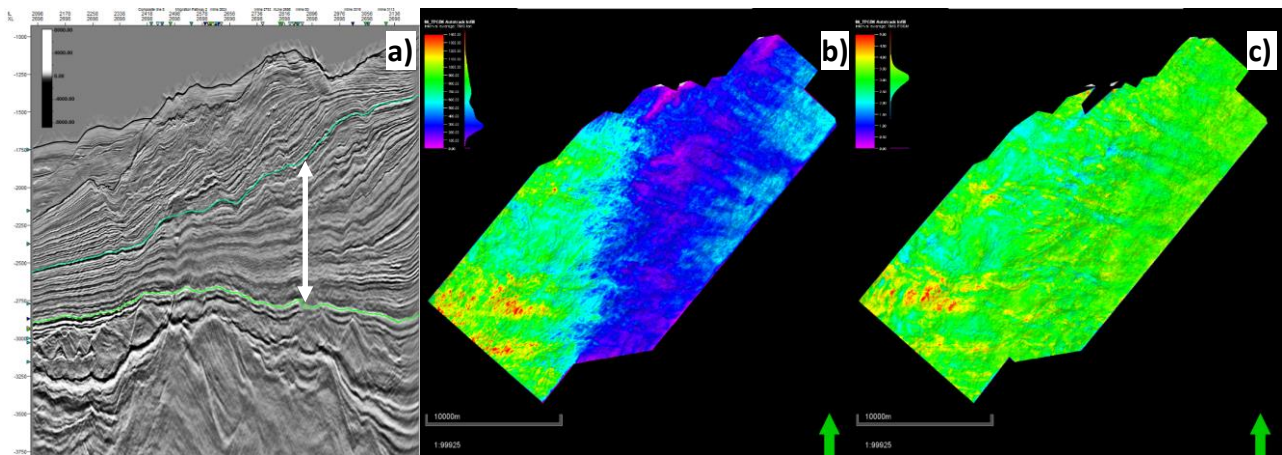


Figure 8. Amplitude integrity testing using an RMS attribute over layer 4 as indicated in panel a). The original PSDM b) shows strongly reduced illumination under the sea floor slump canyons and the prograding Tertiary carbonates, when compared to the geomechanical PSDM c) which shows more uniform illumination for the same interval.

CONCLUSIONS

This study documents the first-time implementation of a method that uses gravity forward modelling to generate a shallow 3D effective pressure (geomechanical) model. We separately studied shallow carbonate and mudstone rock physics, using a novel dataset from the IODP, to conclude that contact models may be more appropriate for converting effective pressures into seismic velocities for shallow imaging applications. The Kraken 3D was re-imaged using the geomechanical velocity model to initiate tomography and sequence-stratigraphic thinking to constrain results in intervals where only minor lateral variations were expected. This helped to focus the tomography on the interval with the strongest lateral velocity variations and ultimately deliver clear improvements in image quality when compared to a traditional approach towards PSDM.

REFERENCES

- Athy, L. F., 1930, Density, porosity, and compaction of sedimentary rocks, AAPG Bull., 14, 1–24.
- Bernecker, T., Kuske, T., Lewis, B., Smith, T., 2015, The hydrocarbon potential of the 2015 Offshore Acreage Release Areas for petroleum exploration, APPEA Journal 55, 71-104.
- Birdus, S., 2008, Restoring velocity variations below seafloor with complex topography by geomechanical modeling. Extended abstracts, 78th Meeting, SEG, Las Vegas.
- Dunne, J., 2016, Kraken 3D – acquisition to interpretation on the edge of the Browse. ASEG Extended Abstracts 2016, 1-8.
- Gallagher, S.J., Fulthorpe, C.S., Bogus, K., and the Expedition 356 Scientists, 2017, Expedition 356 Summary, Proceedings of the International Ocean Discovery Program, Volume 356 Indonesian Throughflow.
- Gibson, H., Fitzgerald, D., Paterson, R., Zengerer, M., 2016, Litho-Constrained Stochastic Inversion of Gravity Gradients, Airborne Gravity Gradiometry workshop, ASEG/PESA/AIG conference, Adelaide.
- Lebedev, M., Pervukhina, M., Mikhaltsevitch V., Dance T., Bilenko, O., and Gurevich B., 2013, An experimental study of acoustic responses on the injection of supercritical CO₂ into sandstones from the Otway Basin, Geophysics, Vol. 78, No. 4, D293–D306.
- Stein, H., 2017, Geological and rock-physical considerations for building shallow elastic property models in deep-marine settings (NW Shelf, Australia), MSc thesis (in press), University of Melbourne.
- Sun, Y. F., 2004, Pore structure effect on elastic wave propagation in rocks: AVO modeling. Journal of Geophysics and Engineering, 1, 268–276.
- Terzaghi K., 1936, The shearing resistance of saturated soils and the angle between the planes of shear, Proc. 1st Conf Soil Mech, 54–56.
- Zengerer, M., 2016, Elvie area, Browse Basin, Western Australia, forward 3D gravity field modelling final report, prepared for Karoon Gas Australia.